2011 / 03 / 28 14 : 38

山本先生，西條先生，皆様

たいへんお世話になっております．
本日，お借りしたP 10 3 台が，陸前高田市の高田病院仮設診療所を中心に活動するチームに向けて送られたことをご報告申し上げます．
これとは別に，エコノミークラス症候群の診療に用いる携帯型エコーについてご助言をお願いします．
地震・津波の発生から17日がたちましたが，岩手では車中泊の患者はあまりいないとされる一方，避難所生活の改善が進まないため，今後，避難所内でのエコノミークラス症候群の発生を心配するという声が，青森県八戸市で診療応援をした弘前大学心臓血管外科から寄せられました．明日から陸前高田市の避難所においてD-ダイマーを含む血液検査が行われることになっており，弘前大学はD-ダイマー高値の住民を中心にエコノミークラス症候群の予防等を進めようとしているようです．実際の患者数など，はっきりしたデータがあるわけでなく，地元の岩手医大の血管グループではまだ対応を決めかねているようです．
そのような段階ですが，エコノミークラス症候群の検出に用いやすい携帯型エコーについての情報と貸し出し（当面2台位）が可能かどうかお教え頂ければ幸甚に存じます．なお，現在お借りしているP 10をこの目的で使うのは難しいというのが，P 10を試してみた岩手医大の血管グループの話です．もし間違っていましたらお詫びします．

小山耕太郎

2011 / 03 / 28 17 : 08

西條先生，高野先生，皆様

早速のご助言ありがとうございました．GEのLogic e等をお借りすることは可能でしょうか？
先ほど荻原様ともお話しさせていただきましたが，お借りしているPhilipsのCX 50には血管用プローブがあり，実際に鮮明な血管エコーを確認していますが，避難所の巡回診療ですので，バッテリーの時間や全体の大きさから，現時点での使用は難しいと判断しています．

小山耕太郎

2011 / 03 / 28 20 : 12

永見様

この度はたいへんご多用のなかいろいろとお力添えを賜りまして，こころよりお礼申し上げます．
携帯型超音波診断機器借用依頼書を添付ファイルでお送りいたします．ご査収下さいますようお願いいたします．
依頼者を全て，「いわて災害医療支援ネットワーク 総括責任者 小林誠一郎」に，借用中の管理者を全て，私，小山耕太郎にしております．ご確認頂ければ幸いです．

小山耕太郎

2011 / 03 / 29 18 : 37

山本先生

岩手医大の小山です．
弘前大学胸部心臓血管外科の谷口先生が岩手県での診療に用いるための携帯型エコーの貸出をお願い申し上げます．
谷口先生としては第一候補にlogiq e 3台を挙げていますが，これが難しいときは，viamoまたはFazone CB，SSD-C 3 CVのなかから使用可能なもの3台をお願いできますでしょうか．
なお，これまでと同様，借用依頼者はいわて災害医療支援ネットワーク，借用中の管理責任者は私，小山としていただければ助かります．

小山耕太郎

2011 / 03 / 30 16 : 58

永井様，皆様

早速お手配いただきありがとうございます．
明日のJALですが，羽田発6：50と15：10のどちらになりますでしょうか．
大学から受け取りに参りますので，決まりましたらお教えください．

谷口先生

装置の到着後，動作の確認と充電，リスト作成を岩手医科大学循環器医療センターで行います．
金曜の午後に盛岡にお入りになるとのことですが，装置は岩手医大でお渡しできればと思います．装置の到着時刻によっては上の作業が金曜午後までかかる可能性があります．ご承知おきいただければと思います．
また，いつから，どの避難所に向かわれるか，いわて災害医療支援ネットワークの高橋智先生とご調整いただければ幸いです．
先生の盛岡入りの日程と装置の搬送については，いわて災害医療支援ネットワークの担当者，赤坂様にお伝えしてあります．
どうかよろしくお願いいたします．

小山耕太郎

2011 / 03 / 31 19 : 08

山本先生，永見様

たいへんお世話になっております．
ただ今，弘前大学谷口先生用の携帯型エコー3台を確かに受領いたしました．
ご多用のなか，迅速にご対応いただきありがとうございました．
明日午前中に動作確認と充電，リスト作成を行い，午後には谷口先生にお渡しできると思います．
取り急ぎご報告申し上げます．

小山耕太郎

Fig. 10 DVTスクリーニング用超音波診断装置の貸与依頼と受け取りの電子メール

ブルエコーの適切な運用を目指し，特に，ニーズと支援のミスマッチを防止すること，あるいは速やかに修正することを心がけました．第一にニーズの確認ですが，発災直後，交通も情報も遮断されたなかで，毎日変化する医療現場のニーズを正確に把握することは困難でした．しかし，岩手県や岩手県医師会，保健所，岩手医大等からの情報をもとに，実際にエコーを使用される先生方からの聞き取り調査を行い，装置の必要性の有無，お届けする装置や探触子の種類を決めることができました．第二は事業の一元的な管理であり，学会本部やいわて災害医療支援ネットワーク，岩手県保健福祉部健康国保課から，メーカーや代理店，そして実際に装置を利用される先生方まで，関係各位のご協力により，情報収集，マッチング，搬送，アフタケアと，一貫した体制で対応することができました．

その後，岩手医大では，いわて災害医療支援ネットワークの経験をもとに，県や医師会と連携した災害時医療体制モデルの確立と人材育成を目指した「災害時地域医療支援教育センター」を開設し，支援活動に必要な超音波診断装置をはじめとする医療機器や種々の物品の備蓄を行っています．(**Fig. 16**)

5. 岩手県の人的被害と医療機関の被災

東日本大震災の死者は19,074人，行方不明者は2,633人で，死因の9割は津波による溺死でした．負傷者は6,219人（重症697人，軽症5,337人，程度不明185人）であり，死者数に対する傷病者数の比（injury-to-death ratio）は0.3でした．岩手県についてみると，死者5,115人，行方不明者1,132人，負傷者211人（重症4人，軽症50人，程度不明157人）で，injury-to-death ratioは0.04でした．阪

2011 / 04 / 22 18 : 53

日本超音波医学会理事長
千田彰一先生

この度は災害の初期から，迅速かつ細やかなご配慮に満ちたご支援を頂きまして，まことにありがとうございました．おかげさまで岩手県の被災地は少しずつではありますが秩序を回復して来ています．県内では今週から学校が再開されたところが多く，久々に聞かれる子供たちの歓声が地域の再建を促してくれるものと喜んでいます．
岩手県の医療ですが，先にお伝えしたように，なかでも基幹となる県立病院が崩壊した陸前高田市と大槌町，山田町の3医療圏で被害が甚大です．県はこの3地域を中心として沿岸各地に仮設診療所を置き，病院や診療所を失った医師達を核にして地域医療の復旧を図りたいと考えています．その復旧過程で，超音波診断装置をはじめとする失った医療機器の回復も重要な課題となっています．そのようななかで，本日，岩手県より私に，現在学会より借用中の9台（当初お借りした6台と，後に弘前大学チーム用としてお借りした3台を合わせ，9台）について，貸与でなく，岩手県への寄贈としていただけないものかとの相談がありました．
装置の現状ですが，先に診療所に貸し出しておりましたP10の5台に加え，私の手元に預かっていたCX50を今週陸前高田市の仮設診療所に送りました．3地域のなかでも医療圏のもっとも大きかった陸前高田市ですが，他の2医療圏に比べると病院機能の回復が早く，先に配布していた携帯型エコーに加えて，より高機能の装置の依頼があったためです．弘前大学用の3装置は，明日4月23日，岩手医大循環器内科のチームが，これも陸前高田地区ですが，避難所でD-ダイマー高値であった住民のスクリーニングに使用します．
貸与頂いている装置は，Siemens Acuson P10（5台），Philips CX50（1台），GE LOGIQe（1台），ALOKA Prosound C3 CV（1台），FUJIFILM FAZONE CB（1台）です．たいへん厚かましいお願いであり，また，各社のご意向もあると存じますが，ご高配を賜りたく，お願い申し上げます．

小山耕太郎

Fig. 11　岩手県からの超音波診断装置の寄贈に関する打診を学会に報告する電子メール

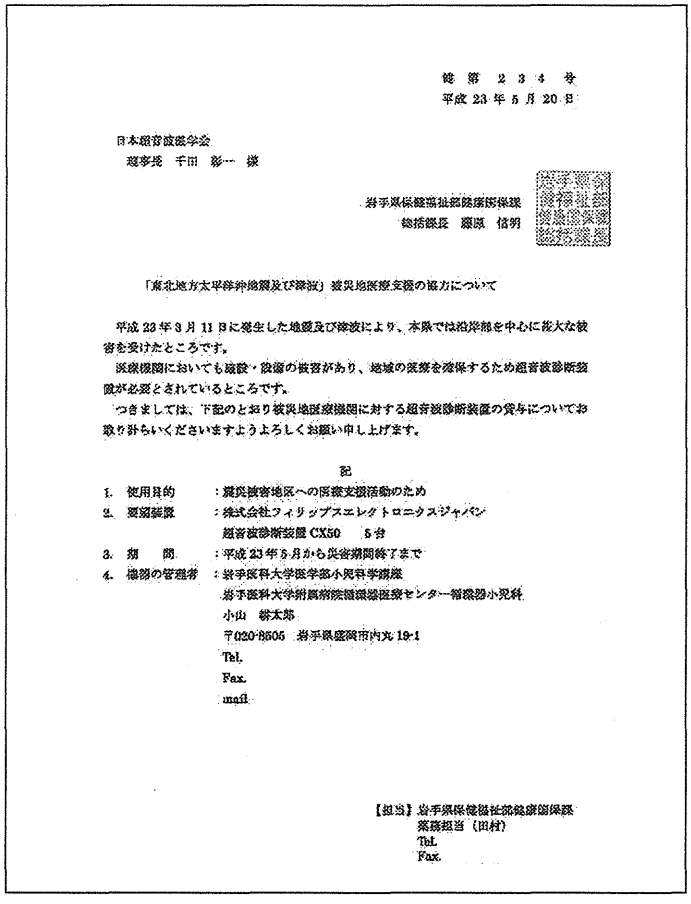

健　第　２３４　号
平成 23 年 5 月 20 日

日本超音波医学会
理事長　千田　彰一　様

岩手県保健福祉部医療国保課
総括課長　藤原　信男

「東北地方太平洋沖地震及び津波」被災地医療支援の協力について

平成 23 年 3 月 11 日に発生した地震及び津波により、本県では沿岸部を中心に甚大な被害を受けたところです。
医療機関においても施設・設備の被害があり、地域の医療を確保するため超音波診断装置が必要とされているところです。
つきましては、下記のとおり被災地医療機関に対する超音波診断装置の貸与についてお取り計らいくださいますようよろしくお願い申し上げます。

記

1. 使用目的　：被災被害地区への医療支援活動のため
2. 要望装置　：株式会社フィリップスエレクトロニクスジャパン
　超音波診断装置 CX50　5台
3. 期　間　：平成 23 年 5 月から災害期間終了まで
4. 機器の管理者　：岩手医科大学医学部小児科学講座
　岩手医科大学附属病院循環器医療センター循環器小児科
　小山　耕太郎
　〒020-8505　岩手県盛岡市内丸 19-1
　Tel.
　Fax.
　mail

【担当】岩手県保健福祉部国保課国保係
　業務担当（田村）
　Tel.
　Fax.

Fig. 12　岩手県保健福祉部国保課から学会への超音波診断装置借用願いの例

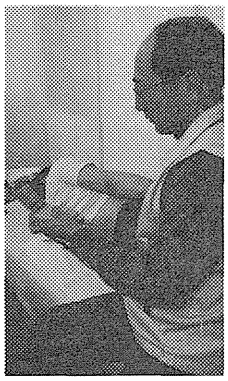

Fig. 13 病院や診療所の先生方による超音波診断装置の利用

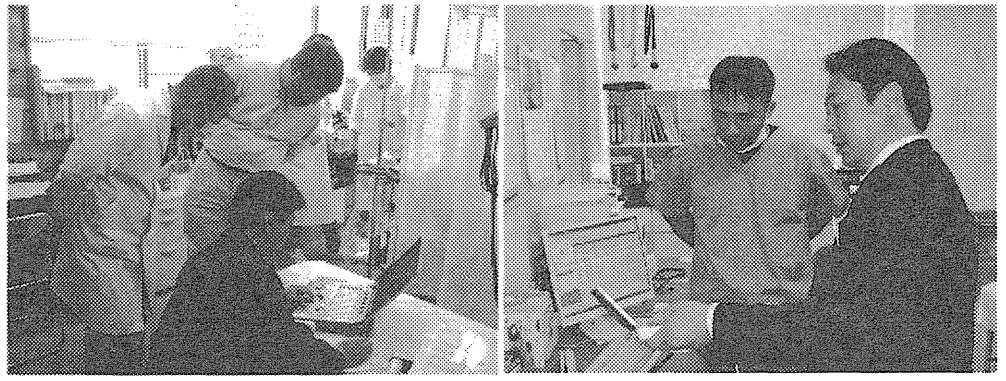

Fig. 14 「いわて災害医療支援ネットワーク」のスタッフや代理店社員等による装置の搬送とメーカー担当者による取扱い説明

（様式3）

医療用具の貸出しに関する確認書

2011年 6月 8日

返却確認日 年 月 日

貸出先 [illegible]（日本超音波医学会）

所在地 [illegible]

貸出し目的

☐デモ ☐臨床試用（有効性・安全性、操作性等の確認） ☒緊急時・災害時対応 ☐事故・故障対応

☐研修 ☐研究目的・公益的研究活動 ☐納期遅延対応 ☐その他

品名・メーカー名・規格型式	数 量	使用者名／設置場所	期 間	症 例 数
超音波診断装置 CX-50 C5-1（腹部プローブ） S5-1（心臓プローブ） L12-3（血管プローブ）	各1式	県立高田病院救急診療所 （未踏ベースキャンプ）	2011/06/08 ～ 災害期間終了	

●貸出し期間中の費用負担：

	貸出し元負担	貸出し先負担
1. 当該医療用具の設置	○	×
2. 輸送	○	×
3. 保守・修理費	○	×
4. 消耗品等	×	○
5. その他の費用	○	×

●貸出し期間が終了した当該医療用具は、速やかに貸出し元に返却する。

医療用具業公正取引協議会

Fig. 15 医療用具業公正取引協議会による医療用具の貸出に関する確認書の例

神・淡路大震災では injury-to-death ratio が 6.8 と，多くの傷病者が発生したのに対して，東日本大震災では死者数に比べ傷病者数が少なく，なかでも岩手県における津波による人的被害の特徴を如実に示しています[3,4]．

当初の予想に反して岩手医大に搬送された患者は少なく，重症例は成人と小児，どちらも津波肺でした[1,5,6]．津波の被災地では，発災後1ヵ月間に後期高齢者を中心に，心不全や心臓突然死，脳梗塞の発症が有意に増加し[7-9]，心不全の発症は津波浸水域の広さや避難所の住民数と関連していました[7]．また，医療機関ならびに医療物資の調達・輸送の障害から，ST上昇型心筋梗塞の患者に対する経皮的冠動脈インターベンションの施行率が有意に減少し，院内死亡率が上昇しました[10]．

岩手県沿岸部の4つの災害拠点病院（県立久慈病院，県立宮古病院，県立釜石病院，県立大船渡病院）は，過去の津波の教訓から，いずれも高台・内陸に新築移転されており，津波被害を免れました．超急性期から傷病者の受け入れが可能で，震災翌日からは入院病床確保のため，沿岸部から内陸部の医療機関へ，小児を含む重症患者等の搬送が行われました．一方，県立山田病院，県立大槌病院，県立高田病院といった災害拠点病院以外の比較的小規模な病院や

2011 / 05 / 23 16 : 19

日本超音波医学会
千田彰一先生，山本一博先生，竹中　克先生
日本超音波医学会事務局
永見哲男　様

たいへんお世話になっております．災害直後から多大なご支援を学会より頂いておりますこと，厚くお礼申し上げます．また，第84回学術集会でご報告の機会をお与えいただきますこと，たいへん光栄に存じます．
岩手県沿岸地域の医療ですが，5月の連休明け頃から，県南部に比べると遅れていた北部の山田地区，大槌地区でも仮設診療所での診療がようやく回復してきております．それに伴い，ご貸与いただいていたエコーも両地区への貸し出しが増えております．
先日は，GE社からVscan 10台を岩手県に寄贈いただきました．各診療所，先生方への聞き取り調査をもとに5月16日から各地への送付を始めております．その際にはGE社の担当の方による使用方法の説明も行われております．また，5月19日にはPhilipsより，CX50をさらに5台，日本超音波医学会を通してご貸与くださると連絡がありました．それもこれも学会のご支援のお陰とこころより感謝しております．CX50につきましては，山田，大槌，陸前高田の3医療圏を中心に使用させていただく方針で現在県と相談を進めております．添付いたしましたのは，岩手県から学会宛にCX50の5台の貸与をお願いする申請書です．ご確認いただければ幸いです．正式には岩手県より学会事務局へ郵送にてお届けいたします．
なお，先にDVTスクリーニング用としてお借りした3台（GE LOGIQe，ALOKA Prosound C3 CV，FUJIFILM FAZONE CB）も，コンベックスとセクターのプローブを各社に追加いただいたうえで，これらの地区の診療所で使用させていただいております．
以上ご報告申し上げます．
学術集会でお会いできるのを楽しみにしております．

小山耕太郎

Fig. 16　医療機関の復旧状況と学会を介して配備された超音波診断装置の利用について報告する電子メール

診療所など57医療機関が大きな被害を受け，医療インフラの再整備，損壊した医療機器の準備やマンパワーの確保など，多くの困難に直面しました[1,2]．

学会を通して岩手県へ貸与または寄贈された装置は，発災後初期には避難所を含む地域の診療に，中期以降には被害を受けた中小の医療機関の再建に重要な役割を果たしました．その後，岩手県が被災医療機関を対象とする補助制度を整備したことから，施設と医療機器に対する一定の補助金を利用することができるようになりました．平成26年1月時点で，医科29，歯科22の医療機関が補助金を活用し，復旧の足がかりとしました[1]．医療機関の復旧に伴い，貸与されていた装置は逐次貸出終了となり，代理店を通して各メーカーに返還されました．

6. おわりに

東日本大震災の初期対応を困難にした最大の要因は通信の途絶でした．そのなかで学会本部と福島，仙台，盛岡が電子メールでつながり，それぞれの情報は不十分ながら，学会のイニシアチブによって情報の集約化と共有化が行われ，迅速な被災地支援が行われました．また，学会本部から被災地の医療現場へと空路，陸路をつないでの超音波診断装置の輸送は，多くの方々と関係諸機関の献身的な協力がなければ実現できませんでした．未曾有の大災害のなか，事業を決断し，その都度状況に応じた最善の決断をして下さった関係者の皆様に改めて心よりお礼申し上げます．

今回の初期対応ならびに中期的支援で明らかになった課題から，将来，電子メールもつながらないような大災害が起こりうることを想定し，多様な通信と輸送の手段を選択できるよう環境整備を進めることが重要と考えます．また，支援物資の調達から，現地での適切な配備と運用，復旧後の回収まで，学会と企業，被災自治体，災害時医療支援本部をつなぐ一連の医療機器の支援体制を構築することが必要です．

利益相反

本論文は，開示する利益相反はありません．

付記：活動記録の参考とするため，本文中に記載された方々の災害時および2015年現在の所属に関し，下記に記載する．

1) 千田彰一先生：当時 日本超音波医学会理事長，香川大学医学部総合診療部教授・(2011年4月－) 病院長，現 日本超音波医学会名誉会員，徳島文理大学副学長・教授，香川大学名誉教授
2) 竹中克先生：当時 日本超音波医学会副理事長，東京大学医学部附属病院検査部講師，現 日本超音波学会理事，日本大学板橋病院循環器内科客員教授
3) 山本一博先生：当時 日本超音波医学会幹事，大阪大学臨床医工学融合研究教育センター特任教授（大阪大学大学院医学研究科循環器内科兼任)，現 日本超音波学会理事，鳥取大学医学部病態情報内科学教授
4) 永見哲男氏：当時・現 日本超音波医学会事務局
5) 高野真澄先生：当時 日本超音波医学会代議員，東北地方会運営委員，福島県立医科大学感染制御・臨床検査医学講座助教，現 日本超音波医学会代議員，東北地方会運営委員，福島県立医科大学集中治療部助教
6) 西條芳文先生：当時・現 日本超音波医学会代議員，東北地方会運営委員，東北大学大学院医工学研究科教授
7) 小山耕太郎：当時・現 日本超音波医学会東北地方会運営委員，岩手医科大学小児科学講座教授

文　献

1) 一般社団法人岩手県医師会編. 東日本大震災の記録 2011.3.11.
2) 細谷光亮，田中総一郎，井田孔明，ほか. 東日本大震災が岩手，宮城，福島の三県の小児と小児医療に与えた被害の実態と，それに対する支援策の効果と問題点についての総括. 日本小児科学会雑誌. 2014;118:1767-4.
3) 消防庁災害対策本部. 平成23年（2011年）東北地方太平洋沖地震（東日本大震災）について（第150報)(平成26年9月10日) http://www.fdma.go.jp/bn/higaihou/pdf/jishin/150.pdf
4) 石川健，小山耕太郎. 大規模災害時の小児救急. 小児科. 2015;56:413-8.
5) Nakadate T, Nakamura Y, Yamauchi K, et al. Two cases of severe pneumonia after the 2011 great east Japan earthquake. Western Pac Surveill Response J. 2012;3:79-82.
6) 赤坂真奈美，荒谷菜海，亀井淳，ほか. 津波肺の管理における真菌の意義. 小児内科. 2014;46:1853-7.
7) Nakamura M, Tanaka F, Nakajima S, et al. Comparisons of the incidence of acute decompensated heart failure before and after the major tsunami in northeast Japan. Am J Cardiol. 2012;110:1856-60.
8) Omama S, Yoshida Y, Ogasawara K, et al. Influence of the great east Japan earthquake and tsunami 2011 on occurrence of cerebrovascular disease in Iwate, Japan. Stroke. 2013;44:1518-24.
9) Niiyama M, Tanaka F, Nakajima S, et al. Population-based incidence of sudden cardiac and unexpected death before and after the 2011 earthquake and thunami in Iwate, northeast Japan. J Am Heart Assoc. 2014;3:e000798 doi:10.1161/JAHA.114.000798.
10) Itoh T, Nakajima S, Tanaka F, et al. Impact of the Japan earthquake disaster with massive tsunami on emergency coronary intervention and in-hospital mortality in patients with acute ST-elevation myocardial infarction. Eur Heart J Acute Cardiovascular Care. 2014;3:195-203.

J Echocardiogr (2015) 13:90–99
DOI 10.1007/s12574-015-0250-8

ORIGINAL INVESTIGATION

Longitudinal systolic strain of the bilayered ventricular septum during the first 72 hours of life in preterm infants

Yurie Nasu[1] · Kotaro Oyama[1] · Satoshi Nakano[1] · Atsushi Matsumoto[1] · Wataru Soda[1] · Shin Takahashi[1] · Shoichi Chida[1]

Received: 19 February 2015 / Revised: 3 June 2015 / Accepted: 21 June 2015 / Published online: 11 July 2015
© Japanese Society of Echocardiography 2015

Abstract
Background Quantitative evaluation of right ventricular myocardial performance in preterm infants remains a challenge because of the limitations of conventional echocardiographic measurement and the complex geometry of the right ventricle (RV). Serial assessment of peak longitudinal systolic strain on the right and left sides of the ventricular septum (VS), RV, and left ventricle (LV) during the transitional period in preterm infants using two-dimensional speckle-tracking echocardiography is reported.
Methods In 21 preterm infants (33 ± 2 gestational weeks, 1,913 ± 218 g birth weight) without mechanical ventilation, inotropic agents, or symptomatic patent ductus arteriosus (PDA), longitudinal strain (LS) was measured on both sides of the VS, RV free wall, and LV, along with conventional echocardiography at 1, 3, 6, 9, 12, 24, 48, and 72 h after birth. Correlations and factors associated with echocardiographic measurements were analyzed.
Result LS was maintained on the four analyzed regions during the first 72 h of life despite significant hemodynamic changes, including a decrease in pulmonary artery pressure and PDA closure. LS was significantly larger on the left side of the VS than on the right side of the VS at 1, 48, and 72 h after birth.
Conclusions Preterm infants showed stable LS on both sides of the VS, the RV free wall, and the LV despite significant hemodynamic changes during the first 72 h of life. These results suggest that the right and left sides of the VS respond differently to the complex cardiopulmonary transitions from fetal to neonatal life in preterm infants.

Keywords Two-dimensional speckle-tracking echocardiography · Strain · Ventricular septum · Preterm infants

Introduction

The transition from fetal to neonatal life is characterized by major circulatory alterations—a decrease in pulmonary vascular resistance, an increase in pulmonary blood flow, and closure of fetal shunts. Preterm infants are susceptible to hemodynamic derangements, such as hypotension and hemodynamically significant patent ductus arteriosus (PDA) during this period [1, 2]. Serial assessment of both right and left ventricular myocardial adaptation during the transition would be helpful for optimal cardiovascular management of preterm infants [1–4]. However, quantitative evaluation of right ventricular myocardial performance in preterm infants remains a challenge because of the limitations of conventional echocardiographic measurement and the complex geometry of the right ventricle (RV). On the other hand, the ventricular septum (VS) is visualized far better than the RV free wall on echocardiography. Furthermore, it has been shown that the VS is a morphologically and functionally bilayered structure divided by a bright line [5–7], and the right and left sides of the VS respond differently to ventricular overload [6].

Until recently, tissue Doppler imaging has been used for noninvasive assessment of myocardial performance, but tissue Doppler measurement is angle-dependent [3, 4]. A novel two-dimensional (2D) speckle-tracking echocardiography, which analyzes grayscale speckle patterns from frame

✉ Yurie Nasu
yurienas@iwate-med.ac.jp

[1] Department of Pediatrics, Iwate Medical University School of Medicine, 19-1 Uchimaru, Morioka, Iwate 020-8505, Japan

to frame based on a pattern matching algorithm and is angle-independent, permits assessment of regional and global myocardial function in the fetus and newborn [8–11]. The accuracy and reproducibility of 2D speckle-tracking have been validated in normal pediatric subjects and patients with congenital heart disease [12].

It has been shown that gestational age, postnatal age and ventricular dimensions all influence myocardial properties measured by tissue Doppler and 2D speckle-tracking echocardiography [3, 4, 8–11]. These findings might reflect developmental characteristics in which the immature myocardium generates less active tension than the mature myocardium at similar muscle lengths [13, 14]. The use of 2D speckle-tracking echocardiography in preterm infants who are ill requires knowledge of the reference values specific to these patient population as well as the variations during the vulnerable transitional period soon after birth. The purpose of the present study was to serially assess myocardial performance of both sides of the VS, RV, and left ventricle (LV) during the transitional period in healthy preterm infants using 2D speckle-tracking echocardiography.

Methods

Study population

Infants weighing 750–2,499 g born in our hospital and admitted to the neonatal intensive care unit from 1 July 2013 to 31 August 2014 were enrolled. Infants meeting the following criteria were excluded—(1) presence of chromosomal abnormality, (2) presence of congenital malformation (brain, heart, digestive tract), (3) small for gestational age, (4) resuscitation by bag and mask or intubation at birth, (5) oxygen administration of FIO_2 >0.3, (6) symptomatic PDA, (7) use of inotropic agents, (8) plethora (hematocrit ≥65 %), severe anemia (hematocrit <35 %), or (9) sepsis (at least one of positive blood culture, immunoglobulin *M* ≥20 mg/dL at birth, or use of immunoglobulin). This study was approved by the institutional review board of Iwate Medical University, after which written consent was obtained from the parents of all subjects prior to enrolment. The subject infants were managed according to standard practices.

Measurement of heart rate, mean blood pressure, respiratory rate, and SpO_2

Heart rate was measured using a heart rate monitor (IntelliVue MP70 Neonatal; Phillips Healthcare, Tokyo, Japan), and mean blood pressure was measured with an indirect oscillometric method (BX-10; Colin, Tokyo, Japan). The respiratory rate was counted visually. SpO_2 was measured with a pulse oximeter (Radical; Masimo, Irvine, CA, USA) attached to the right arm. These recordings were made in combination with echocardiography as described below and stored in a personal computer.

Echocardiographic measurements

Echocardiography was performed in the resting state without sedation by a single experienced investigator (YN) at 1, 3, 6, 9, 12, 24, 48, and 72 h after birth using an ultrasound system (iE33; Phillips Healthcare, Tokyo, Japan) and 7- and 12-MHz sector transducers.

Conventional echocardiographic measurement

According to the American Society of Echocardiography guidelines [15, 16], the following echocardiographic measurements were obtained using M-mode—LV end-diastolic (LVDd) and end-systolic diameters from the parasternal short axis view, and left atrial and aortic root diameters from the parasternal long axis view. LV shortening fraction (LVSF) and left atrial to aortic root (LA/Ao) ratio were obtained. Tricuspid annular plane systolic excursion (TAPSE) was measured from the apical four-chamber view [17]. Right ventricular fractional area change (RVFAC) was obtained using 2D echocardiography from the apical four-chamber view. The time to peak flow (acceleration time, AcT) and right ventricular ejection time (RVET) were measured in the right ventricular outflow tract just below the pulmonary cusp by pulsed Doppler echocardiography in the parasternal short axis view, and AcT/RVET ratio was calculated [18]. Pulsed tissue Doppler imaging for the myocardial performance index (MPI) was obtained at the lateral tricuspid annulus and septal and lateral mitral annuli in the apical four-chamber view [15, 19]. All variables were measured for 3–5 heart beats at each study time, and the mean values were used in the analyses.

2D speckle-tracking echocardiography

The apical four-chamber view was used for measurements of 2D speckle-tracked peak systolic longitudinal strain (LS) of the VS, RV free wall, and LV at frame rates ranging from 101−192, 74−165, and 64−149 frames/s, respectively. All images were recorded after optimizing scan width, gain, and dynamic range to maximize the image quality, and data for one cardiac cycle were stored in an archiving system (QLAB 9.1 software; Philips Healthcare, Tokyo, Japan) for later offline analysis. Care was taken to keep the ultrasound beam aligned parallel to the VS and RV free wall. Images were graded according to the scoring system [20], and only images graded as excellent or good were included in the

following analysis. Regions of interest were manually positioned on the right and left sides of the VS separated by a bright line and the RV free wall, both at the middle part of the wall (Figs. 1, 2a, b). The size of the sampling volume was 7.3 ± 2.0 (mean ± SD) mm for the right side of the VS, 7.3 ± 2.0 mm for the left side of the VS, and 10.9 [10.0–12.4] [median (inter-quartile range)] mm for the RV free wall. For measurement of global LV peak LS, a semi-automatic system traced the endocardial and myocardial borders. Segmental strain is represented by six different color-coded curves, and global LS is represented by the dotted white curve (Fig. 2c). The semi-automatic tracking was visually inspected before accepting the results, and the tracing points were manually repositioned in most cases. Since systolic LS is defined as the percent shortening of the myocardium during systole, more negative LS values indicate more shortening/contraction of the tissue. In the present study, 'LS is larger' when LS values are more negative in intergroup comparisons.

Evaluation of ductus arteriosus and foramen ovale

The ductus arteriosus was observed using color Doppler echocardiography at each time point of the study, and cases were judged patent when continuous ductal shunt flow was

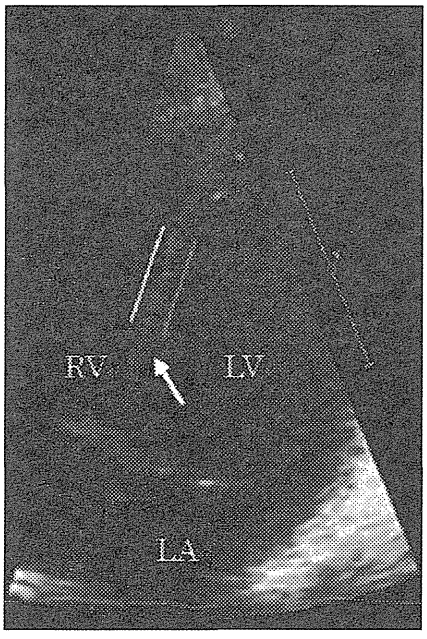

Fig. 1 Apical four-chamber view of the ventricular septum. This four-chamber view shows the *right side* (*yellow*) and the *left side* (*green*) of the ventricular septum separated by the *bright line* (*arrow*). *RV* right ventricle, *LV* left ventricle, *LA* left atrium

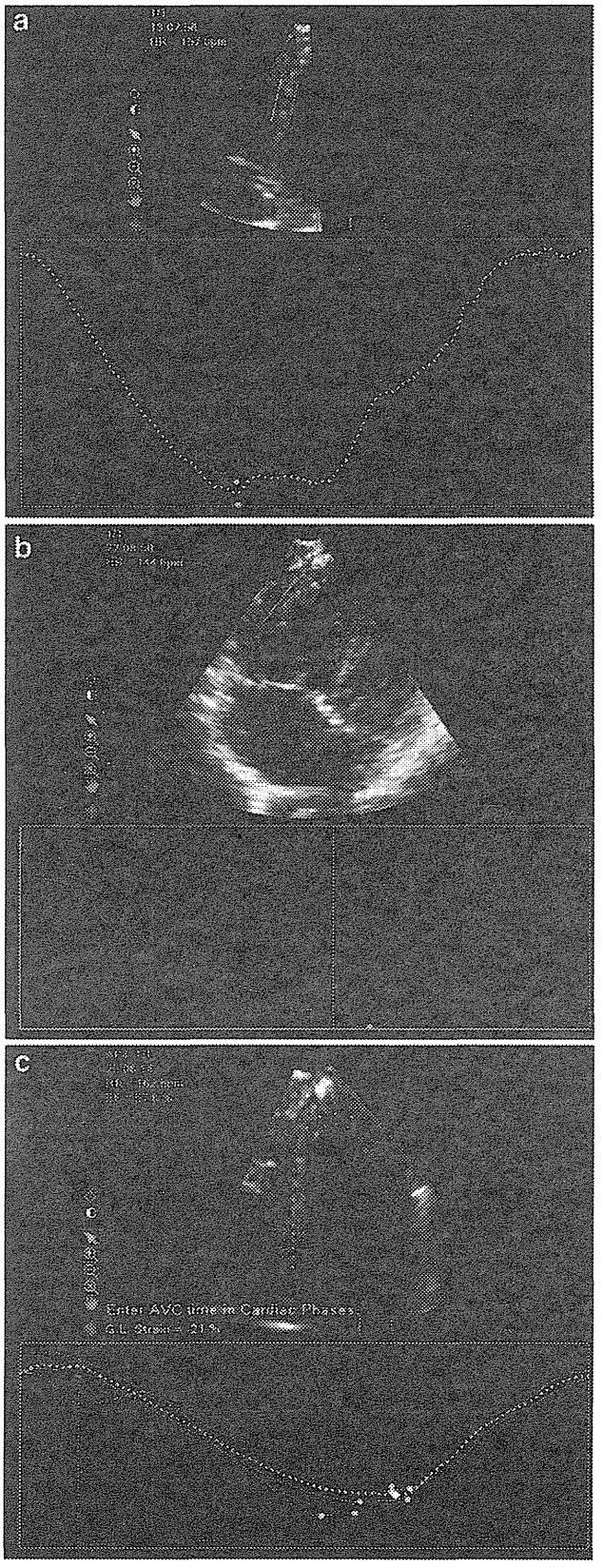

◀**Fig. 2** Apical four-chamber view of the ventricular septum, right ventricular free wall, and global left ventricle. **a** Longitudinal speckle-tracking strain imaging of the *right side* (*yellow*) and *left side* (*green*) of the ventricular septum. **b** Right ventricular free wall longitudinal speckle-tracking strain curve. **c** Left ventricular longitudinal speckle-tracking strain *curve*. Segmental longitudinal strain is graphically represented by six different *color-coded curves*, and global longitudinal strain is graphically represented by the *white dotted curve*

seen from the aorta to the main pulmonary artery. The foramen ovale was judged patent when left to right atrial shunt flow was observed.

Statistical analysis

All data are expressed as mean ± standard deviation (SD) or median [inter-quartile range] according to the data distribution unless otherwise indicated. Analysis of variance with the Tukey correction or Friedman test was performed for intragroup comparisons by time after birth of each type of data as appropriate. The *t* test was used for intergroup comparisons by site and for comparisons between study patients and patients in whom measurements could not be made. To analyze factors associated with echocardiographic measurements, multiple regression analysis was performed with echocardiographic indices at each time after birth as the dependent variable, and sex, gestational age, birth weight, mode of delivery, oxygen administration, use of nasal directional positive airway pressure (n-DPAP), and PDA at each time after birth as independent variables. Conventional echocardiographic measurements affecting LS were analyzed at each time point of the study. Pearson's correlation coefficient was obtained for regional LS values.

The reproducibility of strain measurement was assessed in 10 randomly selected subjects using Bland–Altman plot analysis [bias and 95 % limits of agreement and intraclass correlation coefficient (ICC)]. For intra-observer variability, data were analyzed twice, 8 weeks apart. Interobserver variability was assessed by analyzing data from two separate observers blinded to each other's results. Statistical analysis was performed using SPSS Ver. 20 for Windows (SPSS, Tokyo, Japan) with a significance level of $p < 0.05$ (two-sided).

Results

Characteristics of the patients (Table 1)

Eighty-four preterm, low birth weight infants weighing 750–2,499 g were admitted to our hospital during the study period, and exclusion criteria applied to 49 of them. Of the remaining 35, measurements could not be made for 14 infants because no examiner was present. As a result, the subjects were 21 infants (12 boys, 9 girls), including two sets each of twins and triplets. The gestational age of the subjects was 33 ± 2 weeks (range 28–36 weeks), and birth weight was 1,913 ± 213 g (range 899–2,490 g). Eleven of the 21 subjects were diagnosed with transient tachypnea of the newborn or apnea of prematurity, and oxygen was administered ($FIO_2 \leq 0.3$) within the incubator or an oxygen hood, and nine subjects received n-DPAP within 72 h after birth. No apnea attacks occurred during measurements. There were no differences in clinical characteristics between study patients and the patients in whom measurements could not be made ($n = 14$).

Table 1 Subject characteristics

Variable	Value
Number	21
Gestational week	33 ± 2
Birth weight (g)	1,913 ± 213
Male	12 (57)
Reason of delivery	
PROM	4 (20)
Premature delivery	7 (33)
Premature separation	1 (5)
PIH	2 (9)
Fetal distress	3 (15)
TTTS	2 (9)
Triplet	2 (9)
Mode of delivery	
Vaginal delivery	4 (20)
Caesarean section	17 (80)
Apgar score	
≤7 (1 min)	7 (33)
≤7 (5 min)	2 (9)
O_2 administration ($FiO_2 \leq 0.3$)	11 (52)
n-DPAP	9 (43)

Values indicate mean ± standard deviation or number (%)

PROM premature rupture of the membranes, *PIH* pregnancy-induced hypertension, *TTTS* twin-to-twin transfusion, *n-DPAP* nasal directional positive airway pressure

Changes in heart rate, mean blood pressure, respiratory rate, and SpO_2 over time (Fig. 3)

Heart rate decreased significantly from 163 [154–182] bpm at 1 h to 137 [130–148] bpm at 72 h of age ($p < 0.001$). Mean blood pressure increased significantly from 39 [35–45] mmHg at 1 h to 45 [41–51] mmHg at 72 h of age ($p < 0.01$). Respiratory rate and SpO_2 did not change significantly during the first 72 h of life.

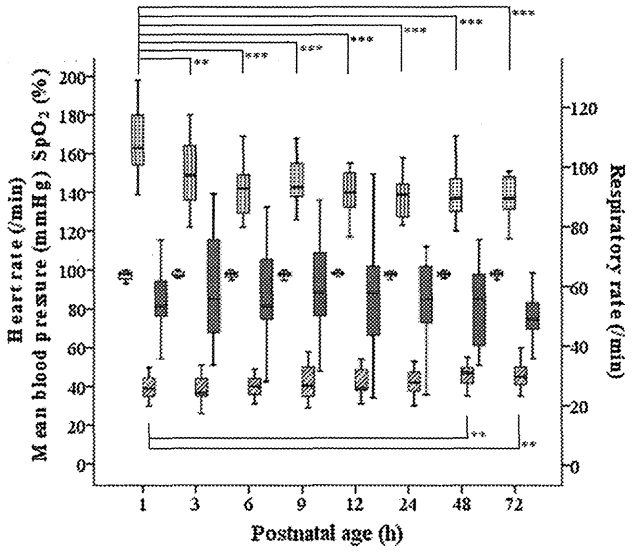

Fig. 3 Changes in heart rate, mean blood pressure, respiratory rate, and SpO_2. The *box* shows the median (*central line*) with interquartile range (25–75th percentile) and the *whisker* represents the 5–95th percentile. *Vertically filled square* heart rate, *diagonally filled square* mean blood pressure, *fully filled square* respiratory rate, *empty filled square* SpO_2. $^{**}p < 0.01$, $^{***}p < 0.001$

Changes in standard echocardiographic measurements (Table 2)

Echocardiography was performed at 1.0 [0.9–1.2] h, 3.0 [3.0–3.2] h, 6.0 [6.0–6.1] h, 9.0 [9.0–9.5] h, 12.0 [11.9–12.3] h, 24.3 [24.0–25.8] h, 48.4 [47.6–49.7] h, and 72.0 [71.5–78.0] h after birth. The LA/Ao ratio decreased significantly from 1.5 ± 0.3 at 1 h to 1.2 ± 0.2 at 9 h ($p = 0.028$), 1.3 ± 0.2 at 24 h ($p = 0.049$), and 1.1 ± 0.2 at 48 h ($p = 0.001$). RVFAC increased from 38.5 ± 9.8 at 1 h to 42.1 ± 8.9 at 48 h ($p = 0.017$), and 47.7 ± 3.6 at 72 h ($p = 0.002$). The AcT/RVET ratio increased significantly from 0.21 ± 0.05 at 1 h to 0.33 ± 0.09 at 24 h ($p = 0.005$), 0.35 ± 0.10 at 48 h ($p < 0.001$), and 0.31 ± 0.10 at 72 h ($p = 0.002$). The LVDd, LVSF and TAPSE did not change during the 72 h after birth. Tissue Doppler-derived MPI at the three measurement points did not change during the study period.

Changes in 2D speckle-tracking strain measurements (Table 2 and Fig. 4)

The bright line was visible in the middle of the VS in the four-chamber view in all subjects. The peak LS on the right side and the left side of the VS and RV free wall did not change during the 72 h after birth. The peak LS was significantly larger on the left side of the VS than on the right side of the VS at 1 h (−22.7 ± 5.7 vs −17.9 ± 4.5 %, $p = 0.047$), 48 h (−19.8 ± 3.1 vs −17.3 ± 4.5 %, $p = 0.048$), and 72 h (−20.9 ± 3.0 vs −14.7 ± 4.6 %, $p = 0.002$). The peak LS remained significantly larger on the RV free wall than on the right side of the VS throughout the study period ($p < 0.01$). The global LV peak LS did not change during the first 72 h of life.

Feasibility and reproducibility of 2D speckle-tracking strain measurements (Table 3)

Strain measurement was feasible in the majority of acquired images—141/150 images (94 %) of the VS, 118/137 images (86 %) of the RV free wall, and 132/144 images (92 %) of the LV. The feasibility of images of the VS was significantly higher compared to that of the RV free wall ($p = 0.01$). For intra-observer reproducibility, Bland–Altman analysis showed minimal bias (<10 %), and the ICC showed moderate to substantial agreement in four strain measurement sites (0.560–0.744). For inter-observer reproducibility, Bland–Altman analysis showed minimal bias (<10 %), and the ICC showed substantial agreement in three speckle-tracking strain measurement sites (0.717–0.758), except the RV free wall, in which the ICC showed modest agreement of 0.455.

Changes in the ductus arteriosus and foramen ovale over time

PDA was seen in 21 infants at 1 h, 18 infants at 3 h, 17 infants at 6 h, 14 infants at 9 h, 13 infants at 12 h, 7 infants at 24 h, 3 infants at 48 h, and 1 infant at 72 h. Compared with 1 h, cases of patency were significantly decreased at 12 h ($p = 0.033$), 24 h ($p < 0.001$), 48 h ($p < 0.001$), and 72 h ($p < 0.001$). Symptomatic PDA was not seen in any case. The left to right shunt through the foramen ovale was observed constantly in all infants during the study period.

Analysis of factors affecting echocardiographic measurements and correlations of regional strain values (Tables 4, 5)

On multiple regression analysis, LVDd and TAPSE appeared significantly associated with birth weight. LVDd was associated with PDA at 12 h and use of n-DPAP at 48 h. Peak LS on the right and left side of the VS was significantly associated with use of n-DPAP in an opposite direction. The associations between peak LS and oxygen administration were inconsistent between the right side of the VS and the RV free wall. The RV free wall peak LS and the global LV peak LS were significantly associated with MPI lateral tricuspid and MPI septal mitral, respectively. The peak LS on the right side of the VS was associated with TAPSE, and the RV free wall peak LS was associated with AcT/RVET. Correlation analysis showed a significant correlation between peak LS on the right side

Table 2 Echocardiographic data during the first 72 h of life

Postnatal age (h)	1	3	6	9
LVDd (cm)	1.6 ± 0.2	1.6 ± 0.2	1.6 ± 0.3	1.5 ± 0.2
LVSF (%)	32.0 [25.3–38.0]	28.0 [26.4–38.8]	28.5 [22.3–36.7]	28.7 [24.0–32.8]
LA/Ao	1.5 ± 0.3	1.3 ± 0.2	1.2 ± 0.3	1.2 ± 0.2*
TAPSE (cm)	0.73 ± 0.10	0.69 ± 0.10	0.71 ± 0.07	0.66 ± 0.07
RVFAC (%)	38.5 ± 9.8	41.4 ± 6.3	31.9 ± 6.9	38.4 ± 8.5
AcT/RVET	0.21 ± 0.05	0.22 ± 0.04	0.27 ± 0.06	0.27 ± 0.09
MPI lateral tricuspid	0.47 ± 0.10	0.44 ± 0.10	0.47 ± 0.06	0.49 ± 0.08
MPI septal mitral	0.54 [0.45–0.70]	0.48 [0.39–0.56]	0.62 [0.57–0.67]	0.54 [0.50–0.58]
MPI lateral mitral	0.46 [0.42–0.54]	0.51 [0.50–0.57]	0.51 [0.40–0.60]	0.51 [0.43–0.61]
VSR peak LS (%)	−17.9 ± 4.5†	−16.2 ± 4.3	−14.6 ± 4.6	−16.3 ± 4.0
VSL peak LS (%)	−22.7 ± 5.7	−17.6 ± 3.4	−16.5 ± 3.9	−19.0 ± 6.9
RVFW peak LS (%)	−22.0 ± 4.7‡	−21.9 ± 5.8‡	−19.3 ± 3.6‡	−22.4 ± 3.0‡
GLV peak LS (%)	−23.8 ± 4.0	−24.2 ± 4.1	−20.4 ± 6.2	−23.0 ± 2.0
Postnatal age (h)	12	24	48	72
LVDd (cm)	1.6 ± 0.2	1.5 ± 0.2	1.5 ± 0.1	1.5 ± 0.3
LVSF (%)	26.9 [25.6–30.8]	31.5 [26.9–37.2]	25.7 [22.8–31.3]	30.0 [28.6–31.5]
LA/Ao	1.2 ± 0.2	1.3 ± 0.2*	1.1 ± 0.2**	1.2 ± 0.3
TAPSE (cm)	0.75 ± 0.09	0.76 ± 0.07	0.70 ± 0.06	0.74 ± 0.10
RVFAC (%)	43.4 ± 5.9	41.5 ± 9.3	42.1 ± 8.9*	47.7 ± 3.6**
AcT/RVET	0.27 ± 0.07	0.33 ± 0.09**	0.35 ± 0.10***	0.31 ± 0.10**
MPI lateral tricuspid	0.44 ± 0.06	0.40 ± 0.12	0.46 ± 0.13	0.41 ± 0.07
MPI septal mitral	0.50 [0.42–0.59]	0.46 [0.38–0.53]	0.43 [0.38–0.53]	0.49 [0.48–0.56]
MPI lateral mitral	0.45 [0.40–0.55]	0.47 [0.41–0.49]	0.54 [0.50–0.60]	0.47 [0.40–0.56]
VSR peak LS (%)	−18.8 ± 3.9	−17.7 ± 4.6	−17.3 ± 4.5†	−14.7 ± 4.6††
VSL peak LS (%)	−22.5 ± 5.4	−21.0 ± 5.1	−19.8 ± 3.1	−20.9 ± 3.0
RVFW peak LS (%)	−21.7 ± 5.0‡	−24.7 ± 4.7‡	−20.8 ± 2.6‡	−22.9 ± 5.1‡
GLV peak LS (%)	−24.9 ± 3.1	−23.4 ± 3.2	−23.8 ± 5.1	−24.9 ± 3.2

Data are presented as mean ± standard deviation or medians (inter-quartile range)

LVDd left ventricular end-diastolic dimension, *LVSF* left ventricular shortening fraction, *LA/Ao* left atrial/aortic root ratio, *TAPSE* tricuspid annular plane systolic excursion, *RVFAC* right ventricular fractional area change, *AcT/RVET* acceleration time/right ventricular ejection time ratio, *MPI* myocardial performance index, *VSR* right side of ventricular septum, *VSL* left side of ventricular septum, *RVFW* right ventricular free wall, *GLV* global left ventricle, *LS* longitudinal strain

* $p < 0.05$, ** $p < 0.01$, *** $p < 0.001$ compared with 1 h after birth

† VSR peak LS compared with VSL peak LS, $p < 0.05$

†† VSR peak LS compared with VSL peak LS, $p < 0.01$

‡ VSR peak LS compared with RVFW peak LS, $p < 0.01$

VS and on the RV free wall at 72 h ($r = 0.593$, $p < 0.001$), and peak LS on the left side of the VS and on the global LV at 72 h ($r = 0.55$, $p = 0.007$).

Discussion

In the present study, peak LS was maintained at the four analyzed regions during the first 72 h of life despite significant hemodynamic changes, including decreased heart rate and increased mean blood pressure, and decreased pulmonary artery pressure and PDA closure as assessed by conventional echocardiography. The peak LS was significantly larger on the left side of the VS than on the right side of the VS at 1, 48, and 72 h after birth. To the best of our knowledge, this is the first report of serial measurement of systolic LS on both sides of the VS, RV, and LV in preterm infants using 2D speckle-tracking echocardiography.

There are few studies of 2D speckle-tracking echocardiography examining fetal or neonatal myocardial

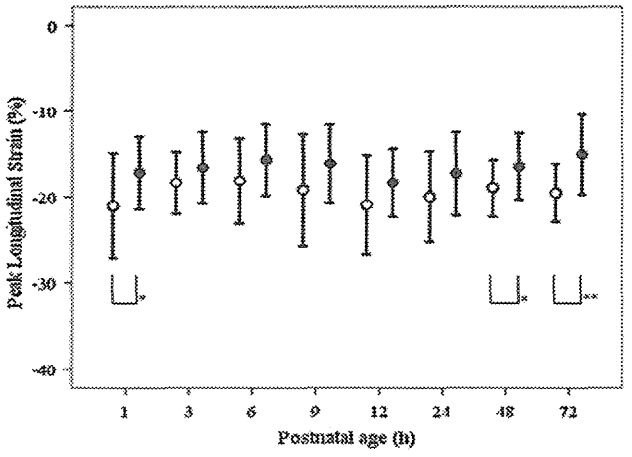

Fig. 4 Changes in 2D speckle-tracking strain measurements on the *right side* and the *left side* of the ventricular septum. The peak longitudinal strain is significantly larger on the *left side* than on the *right side* of the ventricular septum at 1, 48, and 72 h after birth. The *bar* shows the mean ± standard deviation. *Fully filled circle*, *right side* of the ventricular septum; *empty filled circle*, *left side* of the ventricular septum. $*p < 0.05$, $**p < 0.01$

performance. In normal fetuses, Di Salvo et al. [8] studied LS in RV, VS and LV during 20–32 weeks of gestation and found significant correlations between gestational age and LS ($n = 100$). In healthy term infants, Schubert et al. [9] found that LS values at a mean 170 (range 135–207) h after birth were significantly larger in the RV than in the LV and VS ($n = 30$). These values were significantly decreased compared to fetal values of the same infants at 28 weeks of gestation. Jain et al. [10] reported that RV free wall LS was maintained between 15 ± 2 h and 35 ± 2 h of age in healthy term newborns ($n = 50$). In preterm infants, Levy et al. [11] reported high feasibility and reproducibility of RV LS measurement in 50 infants with 27 ± 1 gestational weeks and 0.96 ± 0.2 kg birth weight at 32 weeks (1.42 ± 0.3 kg body weight) and at 36 weeks postmenstrual age (2.21 ± 0.3 kg body weight), but exact values and comparisons between LS measurements at two time points were not included. Using tissue Doppler imaging, it has been found that LS of the VS, RV, and LV did not change between 10 and 45 h post-delivery in 54 preterm infants with a median gestation and birth weight of 26.5 weeks and 915 g, respectively. All infants in this study received early surfactant prior to the first echocardiography, 61 % received mechanical ventilation, and all infants had large unconstricted PDA at 10 h of age [4]. The results of the present study and those of previous studies [4, 9, 10] might indicate that abrupt changes in LS occur at the time of cord clumping and removal of the placenta and that LS is maintained at the VS, RV, and LV to some extent despite significant hemodynamic changes during the transition period in preterm infants. This study reveals that the peak LS of the VS, RV, and LV is relatively independent of hemodynamic changes and can therefore serve as an index for myocardial evaluation during the transition in preterm infants.

Longitudinal deformation was significantly larger on the left side of the VS than on the right side of the VS at 1, 48, and 72 h after birth. This is contrary to previous findings from normal subjects [5, 7]. Boettler et al. [5] found similar LS on the right and on the left VS in healthy adults ($n = 30$, age range 18–53 years) using Doppler myocardial imaging. Hayabuchi et al. [7] reported similar findings in normal children ($n = 132$, age range 1.0–10.0 years) using 2D speckle-tracking echocardiography. They speculated

Table 3 Intra-observer and inter-observer variabilities

	1st Mean ± SD	2nd Mean ± SD	*p* value	Bias (95 % LOA)	ICC
Intra-observer variability					
VSR peak LS (%)	−18.5 ± 4.2	−18.3 ± 4.3	0.919	0.2 (−7.9 to 8.3)	0.560
VSL peak LS (%)	−20.9 ± 4.4	−20.0 ± 3.8	0.628	0.9 (−4.9 to 6.7)	0.744
RVFW peak LS (%)	−23.3 ± 3.6	−21.9 ± 3.6	0.389	1.4 (−4.3 to 7.1)	0.628
GLV peak LS (%)	−26.0 ± 2.2	−24.7 ± 2.8	0.263	1.3 (−1.5 to 4.0)	0.739
	Observer 1 Mean ± SD	Observer 2 Mean ± SD	*p* value	Bias (95 % LOA)	ICC
Inter-observer variability					
VSR peak LS (%)	−18.3 ± 4.3	−17.4 ± 3.1	0.576	1.0 (−4.1 to 6.0)	0.758
VSL peak LS (%)	−20.0 ± 3.8	−20.4 ± 3.0	0.814	−0.4 (−5.6 to 4.9)	0.717
RVFW peak LS (%)	−21.9 ± 3.6	−21.0 ± 4.5	0.604	1.0 (−7.5 to 9.4)	0.455
GLV peak LS (%)	−24.7 ± 2.8	−25.2 ± 3.7	0.736	−0.5 (−4.9 to 4.0)	0.717

VSR right side of ventricular septum, *VSL* left side of ventricular septum, *RVFW* right ventricular free wall, *GLV* global left ventricle, *LS* longitudinal strain, *LOA* limits of agreement, *ICC* intraclass correlation coefficient

Table 4 Clinical factors affecting echocardiographic measurements

Postnatal age (h)	Dependent variable	Independent variable	β	p	R^2
1	TAPSE	Birth weight	0.921	<0.001	0.734
6	GLV peak LS	Use of n-DPAP	0.59	0.002	0.630
	RVFW peak LS	O_2 administration	0.729	0.002	0.495
12	LVDd	Birth weight	0.636	0.001	0.534
		PDA	0.495	0.005	0.534
48	LVDd	Use of n-DPAP	−0.525	0.004	0.536
	VSR peak LS	Use of n-DPAP	−0.498	0.018	0.514
		O_2 administration	−0.728	0.002	0.514
72	LVDd	Birth weight	0.769	<0.001	0.568
	VSL peak LS	Use of n-DPAP	0.616	0.014	0.325

β standardized coefficient, R^2 coefficient of determination, *TAPSE* tricuspid annular plane systolic excursion, *RVFW* right ventricular free wall, *VSR* right side of ventricular septum, *VSL* left side of ventricular septum, *LVG* global left ventricle, *LS* longitudinal strain, *n-DPAP* nasal directional positive airway pressure, *PDA* patent ductus arteriosus

Table 5 Conventional echocardiographic measurements affecting speckle-tracking echocardiographic measurements

Postnatal age (h)	Dependent variable	Independent variable	β	p	R^2
1	GLV peak LS	MPI septal mitral	1.017	<0.001	0.827
	VSR peak LS	TAPSE	−0.749	0.002	0.525
	RVFW peak LS	MPI lateral tricuspid	0.583	0.029	0.285
6	GLV peak LS	MPI septal mitral	0.498	0.047	0.378
12	RVFW peak LS	AcT/RVET	0.534	0.033	0.235

β standardized coefficient, R^2 coefficient of determination, *GLV* global left ventricle, *VSR* right side of ventricular septum, *RVFW* right ventricular free wall, *LS* longitudinal strain, *MPI* myocardial performance index, *TAPSE* tricuspid annular plane systolic excursion, *AcT/RVET* acceleration time/right ventricular ejection time ratio

that the close connection of both sides of the VS prevented independent longitudinal movement, and each side affected the other. Interestingly, however, Hayabuchi et al. [6] documented in another report that in patients ($n = 22$, age 9.0 ± 4.2 years) with a hemodynamically significant atrial septal defect, LS on both sides of the VS was significantly larger than in controls. Furthermore, LS on the left side of the VS was significantly larger than on the right side of the VS.

A geometric model showed that the right and left sides of the VS respond differently to various conditions [21]. At birth, the systemic vascular resistance abruptly increases with discontinuation of the low-resistance placental circulation. Data for right ventricular preload are less conclusive, but it seems that preload drops with clamping of the umbilical cord and rises within hours to supra-fetal levels [9]. The rapid decrease in pulmonary vascular resistance and the increase in pulmonary blood flow augments preload to the left side of the heart. The increased ductal left-to-right shunt also enhances venous return to the left atrium, which will raise left atrial pressure. If the foramen ovale is patent, an atrial left-to-right shunt may raise right ventricular output to levels above those of systemic venous return [14, 22]. All subjects in the present study had a patent foramen ovale until 72 h of age. Although the magnitude of the shunt was not quantified, both ductal and atrial shunts might have caused a significant right ventricular volume overload and affected LS of the VS along with left ventricular pressure and volume overload. It is also plausible that inotropic stimulation with the catecholamine surge induced by delivery affects strain measurements immediately after birth. During the following days, the loading conditions of the right and left ventricles further changed along with a further decrease in pulmonary vascular resistance and closure of the ductal shunt. All these responses might have altered the myocardial performance of the RV and LV and affected the longitudinal deformation of the VS. The different deformation between the bilayered VS might indicate the presence of the delicate pressure and volume adaptation, which is not shown on the RV free wall and global LV deformation.

The peak LS on the right and left sides of the VS was significantly associated with use of n-DPAP at 48 and 72 h, respectively, in an opposite direction. The global LV peak LS and LVDd were also significantly associated with use of n-DPAP at 6 and 48 h, respectively. To our knowledge,

the impact of n-DPAP on myocardial deformation in preterm infants was not addressed previously. In adult patients with obstructive sleep apnea, a few studies demonstrated that chronic therapy using n-DPAP improved both right and left ventricular LS [23, 24]. However, the mechanisms by which n-DPAP alter the hemodynamic status of patients are complex. It has been shown that incremental positive end-expiratory pressure affects the right and left ventricular LS differently and results in a change in right and left ventricular dimensions inversely in adult patients [25]. Since there were significant correlations between LS on the right side of the VS and the RV free wall and between LS on the left side of the VS and global LV at 72 h after birth, the present results suggest that the right and left sides of the VS respond differently to the multiple and complex cardiopulmonary transitions from fetal to neonatal life in preterm infants and that peak LS on the right and left sides of VS might be a sensitive parameter to detect subtle changes in regional myocardial performance in patients with n-DPAP.

The feasibility and reproducibility of 2D strain measurement in the present study were in agreement with previous studies [6–11, 26], but feasibility was lower for the RV free wall than for the VS. For inter-observer reproducibility, the ICC showed substantial agreement on both sides of the VS and the LV, whereas the ICC for the RV free wall was modest. These results might be related to the method of image acquisition of the RV; a standard apical four-chamber view was used in order to avoid interfering with respiration of small infants. The RV myofiber architecture is characterized by dominant longitudinal layers aligned from the base to apex, which allow greater longitudinal than radial shortening and twisting and rotational movements [10]. It is important to define the full extent of the RV free wall to avoid the loss of the optimum number of RV segments through the cardiac cycle for tracking the longitudinal movement [10, 27]. The standard apical four-chamber view might have failed to include the entire RV free wall in its imaging plane and led to poor speckle-tracking. Recently, an RV-focused view has been advocated for high clinical feasibility and reproducibility [10, 15].

Study limitations

Several study limitations should be addressed. First, this study included a small number of infants in a single center, and a larger study is needed to determine the myocardial response during the transitional period in preterm infants. Second, a standard apical four-chamber view was used and not a RV-focused view or any other view, which might have affected LS measurements of the RV free wall. Third, the focus was on mid-ventricular regions of the VS and RV free wall. The myofibers in the base and mid regions of the VS have longitudinal orientation, and the fibers of its apex have circumferential orientation, according to Torrent-Guasp et al. [28]. A recent meta-analysis showed a significant base to apex segmental strain gradient in the RV free wall in normal children [29]. Comparisons with strain values from different regions are necessary to determine the global myocardial performance in preterm infants. Fourth, in this study, we measured the LS and analyzed its correlation with clinical and conventional echocardiographic characteristics. However, the circumferential strain of both sides of VS might have the different pattern in this period. Hayabuchi et al. [6] reported that the longitudinal deformation of both sides of VS was similar in normal children, whereas circumferential strain was significantly different. Finally, a commercially available ultrasound system and vendor-customized software, which are different from those used in most previous pediatric studies, were used [8–10]. Since strain measurements are reported to be significantly different for each of the vendors [30], care should be taken when comparing results between studies.

Conclusion

Preterm infants without mechanical ventilation, inotropic agents, or symptomatic PDA showed stable LS on both sides of the VS, RV free wall, and LV despite hemodynamically significant changes during the first 72 h of life. LS was significantly larger on the left side of the VS than on the right side of the VS at 1, 48, and 72 h after birth, and the responsible mechanisms and clinical implications should be elucidated in further studies.

Acknowledgment This study was approved by the institutional review board of Iwate Medical University (H25-63).

Conflict of interest Yurie Nasu, Kotaro Oyama, Satoshi Nakano, Atsushi Matsumoto, Wataru Soda, Shin Takahashi, and Shoichi Chida declare that they have no conflict of interest.

Human rights statement and informed consent All procedures followed were in accordance with the ethical standards of the institutional review board of Iwate Medical University and with the Helsinki Declaration of 1975, as revised in 2000. Informed consent was obtained from the parents of all subjects prior to enrolment.

References

1. Kluckow M, Seri I. Clinical presentations of neonatal shock: the very low birth weight neonate during the first postnatal day. In: Kleinman CS, Seri I, Polin RA editors. Hemodynamics and Cardiology. Neonatology Questions and Controversies. 2nd ed. Philadelphia, Elsevier Saunders; 2012. pp. 237-67.

2. El-Khuffash AF, Jain A, Dragulescu A, et al. Acute changes in myocardial systolic function in preterm infants undergoing patent ductus arteriosus ligation: a tissue Doppler and myocardial deformation study. J Am Soc Echocardiogr. 2012;25:1058–67.
3. Lee A, Nestaas E, Liestol K, et al. Tissue Doppler imaging in very preterm infants during the first 24 h of life: an observational study. Arch Dis Child Fetal Neonatal Ed. 2014;99:F64–9.
4. James AT, Corcoran JD, Jain A, et al. Assessment of myocardial performance in preterm infants less than 29 weeks gestation during the transitional period. Early Hum Dev. 2014;90:829–35.
5. Boettler P, Claus P, Herbots L, et al. New aspects of the ventricular septum and its function: an echocardiographic study. Heart. 2005;91:1343–8.
6. Hayabuchi Y, Sakata M, Ohnishi T, et al. A novel bilayer approach to ventricular septal deformation analysis by speckle tracking imaging in children with right ventricular overload. J Am Soc Echocardiogr. 2011;24:1205–12.
7. Hayabuchi Y, Sakata M, Kagami S. Assessment of the helical ventricular myocardial band using standard echocardiography. Echocardiography. 2014. doi:10.1111/echo.12624.
8. Di Salvo G, Russo MG, Paladini D, et al. Two-dimensional strain to assess regional left and right ventricular longitudinal function in 100 normal fetuses. Eur J Echocardiogr. 2008;9:754–6.
9. Schubert U, Müller M, Norman M, et al. Transition from fetal to neonatal life: changes in cardiac function assessed by speckle-tracking echocardiography. Early Hum Dev. 2013;89:803–8.
10. Jain A, Mohamed A, El-Khuffash A, et al. A comprehensive echocardiographic protocol for assessing neonatal right ventricular dimensions and function in the transitional period: normative data and Z scores. J Am Soc Echocardiogr. 2014;27:1293–304.
11. Levy PT, Holland MR, Sekarski TJ, et al. Feasibility and reproducibility of systolic right ventricular strain measurement by speckle-tracking echocardiography in premature infants. J Am Soc Echocardiogr. 2013;26:1201–13.
12. Singh GK, Cupps B, Pasque M, et al. Accuracy and reproducibility of strain by speckle tracking in pediatric subjects with normal heart and single ventricular physiology: a two-dimensional speckle-tracking echocardiography and magnetic resonance imaging correlative study. J Am Soc Echocardiogr. 2010;23:1143–52.
13. Friedman WF. The intrinsic physiologic properties of the developing heart. Prog Cardiovasc Dis. 1972;15:87–111.
14. Rudolph AM. Congenital diseases of the heart. Clinical-physiological considerations. 3rd ed. West Sussex: Wiley-Blackwell: 2009.
15. Rudski LG, Lai WW, Afilalo J, et al. Guidelines for the echocardiographic assessment of the right heart in adults: a report from the American Society of Echocardiography. Endorsed by the European Association of Echocardiography, a registered branch of the European Society of Cardiology, and the Canadian Society of Echocardiography. J Am Soc Echocardiogr. 2010;23:685–713.
16. Mertens L, Seri I, Marek J, et al. Targeted neonatal echocardiography in the neonatal intensive care unit: practice guidelines and recommendations for training. Writing group of the American Society of Echocardiography (ASE) in collaboration with the European Association of Echocardiography (EAE) and the Association for European Pediatric Cardiologists (AEPC). J Am Soc Echocardiogr. 2011;24:1057–78.
17. Koestenberger M, Ravekes W, Everett AD, et al. Right ventricular function in infants, children and adolescents: reference value of the tricuspid annular plane systolic excursion (TAPSE) in 640 healthy patients and calculation of z score values. J Am Soc Echocardiogr. 2009;22:715–9.
18. Kitabatake A, Inoue M, Asao M, et al. Noninvasive evaluation of pulmonary hypertension by a pulsed doppler technique. Circulation. 1983;68:302–9.
19. Mejia AAS, Simpson KE, Hildebolt CF, et al. Tissue Doppler septal Tei index indicates severity of illness in pediatric patients with congestive heart failure. Pediatr Cardiol. 2014;35:411–8.
20. Colan SD, Shirali G, Margossian R, et al. The ventricular volume variability study of the pediatric heart network: study design and impact of beat averaging and variable type on the reproducibility of echocardiographic measurements in children with chronic dilated cardiomyopathy. J Am Soc Echocardiogr. 2012;25:842–54.
21. Beyar R, Dong SJ, Smith ER, et al. Ventricular interaction and septal deformation: a model compared with experimental data. Am J Physiol. 1993;265:2044–56.
22. Evans N, Iyer P. Assessment of ductus arteriosus shunt in preterm infants supported by mechanical ventilation: effect of interatrial shunting. J Pediatr. 1994;125:778–85.
23. Haruki N, Takeuchi M, Kanazawa Y, et al. Continuous positive airway pressure ameliorates sleep-induced subclinical left ventricular systolic dysfunction: demonstration by two-dimensional speckle-tracking echocardiography. Eur J Echocardiogr. 2010;11:352–8.
24. Hammerstingl C, Schueler R, Wiesen M, et al. Impact of untreated obstructive sleep apnea on left and right ventricular myocardial function and effects of CPAP therapy. PLoS ONE. 2013. doi:10.1371/journal.pone.0076352.
25. Franchi F, Faltoni A, Cameli M, et al. Influence of positive end-expiratory pressure on myocardial strain assessed by speckle tracking echocardiography in mechanically ventilated patients. BioMed Res Int. 2013. doi:10.1155/2013/918548.
26. Fukuda Y, Tanaka H, Sugiyama D, et al. Utility of right ventricular free wall speckle-tracking strain for evaluation of right ventricular performance in patients with pulmonary hypertension. J Am Soc Echocardiogr. 2011;24:1101–8.
27. Giusca S, Dambrauskaite V, Scheurwegs C, et al. Deformation imaging describes right ventricular function better than longitudinal displacement of the tricuspid ring. Heart. 2010;96:281–8.
28. Torrent-Guasp F, Ballester M, Buckberg GD, et al. Spatial orientation of the ventricular muscle band: physiologic contribution and surgical implication. J Thorac Cardiovasc Surg. 2001;122:389–92.
29. Levy PT, Mejia AAS, Machefsky A, et al. Normal ranges of right ventricular systolic and diastolic strain measures in children: a systematic review and meta-analysis. J Am Soc Echocardiogr. 2014;27:549–60.
30. Takigiku K, Takeuchi M, Izumi C, et al. Normal range of left ventricular 2-dimensional strain: Japanese Ultrasound Speckle Tracking of the Left Ventricle (JUSTICE) study. Circ J. 2012;76:2623–32.

厚生労働科学研究費補助金　地域医療基盤開発推進研究事業

持続可能な広域医療情報連携ネットワークシステムの構築に関する研究
平成 27 年度　総合研究報告書

発行日　平成 28 年 3 月
発行者　岩手医科大学　小川　彰
〒020-8505　岩手県盛岡市内丸 19－1
TEL 019－651－5111（代）
発行所　　株式会社杜陵印刷